Preparation, adsorptive properties and chemical regeneration studies of high-porous activated carbon derived from *Platanus orientalis* leaves for Cr(VI) removal

Xiaowei Liu, Lihui Huang, Lisha Wang, Chuang Wang, Xueyuan Wu, Guihua Dong and Yangyang Liu

ABSTRACT

Activated carbon (AC) was prepared from *Platanus orientalis* leaves by H_3PO_4 activation using a microwave heating method and characterized by SEM (scanning electron microscopy), Brunauer–Emmett–Teller (BET) surface area analysis and FTIR (Fourier transform infrared spectroscopy) techniques. AC exhibited a surface area of 1089.67 m^2/g and a relatively high pore volume of 1.468 cm^3/g. Utilization of AC for the removal of Cr(VI) from aqueous solution was researched. The adsorption efficiency was highly pH dependent and adsorption capacity of AC for Cr(VI) could reach up to 135.24 mg/g. Adsorption equilibrium could be quickly reached within 2 h. A kinetic study indicated that the adsorption of Cr(VI) conformed to the pseudo-second-order model ($R^2 > 0.99$). An intraparticle diffusion model was applied to describe the adsorption kinetics, and the results showed that there are other factors that affect the rate. Chemical regeneration for AC saturated with Cr(VI) was performed and HNO_3 displayed the best regeneration performance among the four chemical regeneration agents (HNO_3, H_2SO_4, NaOH, NaCl). The regeneration performance increased at first and then decreased with the rise of HNO_3 concentration, and regeneration reaction could reach equilibrium within 4 h in the first cycle. The FTIR spectra revealed that HNO_3 successfully introduced N-H bonds onto the AC surface in the regeneration process.

Key words | activated carbon, Cr(VI), microwave heating, *Platanus orientalis* leaves, regeneration

Xiaowei Liu
Lihui Huang (corresponding author)
Lisha Wang
Chuang Wang
Xueyuan Wu
Guihua Dong
Yangyang Liu
School of Environmental Science and Engineering,
Shandong University,
No. 27, Shandanan Road, Jinan 250100,
Shandong,
China
E-mail: *huanglihui409@126.com*

INTRODUCTION

Chromium is widely used in various industries, including metallurgy, mineral, electroplating, tanning, dye and so on. Herein, large amounts of waste-water containing chromium, which is degradation-resistant, highly toxic and highly carcinogenic, is being produced annually. Both of the two forms of chromium, hexavalent chromium (Cr(VI)) and trivalent chromium (Cr(III)), are oxidation states in aqueous systems (Ihsanullah *et al.* 2016), but the former is much more toxic than the latter; thus Cr(VI) has always gained more attention from researchers. Because of the high surface area, developed porosity, abundant functional groups and stable physicochemical properties of activated carbons (ACs), adsorption by ACs has been one of the most frequently used methods among the numerous technologies to remove Cr(VI) from waste-water. However, as a result, a mass of AC saturated with Cr(VI) has been abandoned, which will bring about a waste of resources and secondary pollution. Therefore, it is imperative to explore the regeneration (desorption) technologies of ACs containing high concentrations of Cr(VI).

There are mainly two mechanisms for the regeneration of spent AC: (1) destroying the interaction force between

doi: 10.2166/wh.2018.068

adsorbate molecule and AC surface; and (2) destroying the porous structure of AC so as to remove the adsorbate. Traditional regeneration technologies of spent AC include thermal regeneration, chemical regeneration (Li *et al.* 2015), biologic regeneration (Oh *et al.* 2015), ultrasonic regeneration (Liu *et al.* 2017), etc., while microwave regeneration (Mao *et al.* 2015), photocatalytic regeneration (Chen *et al.* 2016), etc., are new-style regeneration methods. Each of the above-mentioned regeneration methods has pros and cons; thermal and chemical regeneration are the most frequently used regeneration methods. Yet there is a shortage of relevant information on chemical regeneration of Cr(VI) saturated AC in the literature.

Many kinds of low-cost waste biomass have been used as precursors for AC preparation, such as sugarcane bagasse (Kaushik *et al.* 2017), coconut husk (Aljeboree *et al.* 2017) and orange peel (Köseoğlu & Akmil-Başar 2015), but the adsorption capacity of these ACs is not ideal. *Platanus orientalis* is widely planted in Eurasia, especially in China, as an important ornamental and economic plant. In China, *Platanus orientalis* spreads almost all over every city and town; thereby a tremendous quantity of *Platanus orientalis* dead leaves (POLs) are produced annually. However, quite a large number of the POLs are not disposed of properly, such as in the vast rural areas of China; most of them are simply burned up in winter. Herein, there is a special and practical significance to find a preferable disposal method for POLs in China. POLs consist of ample leaf vascular cylinders and developed stomata, which are beneficial for preparing efficient ACs. However, as far as we know, few works have been carried out to employ POLs to prepare AC thus far. In the present study, POLs were employed as precursor, H_3PO_4 as activator, and microwave heating as calcination craft to produce AC. Compared with conventional heating methods, microwave thermal treatment has the advantages of fast temperature rise, homogeneous temperature distribution and saving of energy (Yang *et al.* 2010). The carbon was characterized by means of scanning electron microscopy (SEM), Brunauer–Emmett–Teller (BET) surface area analysis and Fourier transform infrared spectroscopy (FTIR). Then batch adsorption experiments toward Cr(VI) were conducted and sorption isotherm and kinetics were studied. Additionally, the regeneration processes were carried out using four different types of chemical regeneration agents to explore the regeneration rates, and the best one was chosen to discuss the regeneration mechanism. Eventually, the Cr(VI) in regeneration solution was converted to barium chromate precipitate.

MATERIALS AND METHODS

Reagents

H_3PO_4 (85%, China), potassium dichromate ($K_2Cr_2O_7$, 99.8%), H_2SO_4, HCl, HNO_3, NaOH, NaCl, $BaCl_2$, and 1,5-diphenylcarbazide were purchased from Shanghai Hushi Laboratorial Equipment Co., Ltd (Shanghai, China).

All the reagents were analytical grade, and all the water used in the experiment was distilled water.

Preparation and characterization of POLs-based activated carbon

POLs collected from Jinan city (Shandong, China) were mixed with 40 wt% H_3PO_4 with the optimum mass ratio of 1:3, and heated to 450 °C in a microwave oven (MKX-M1-Q, Qingdao) for 20 min. Afterwards the material was washed with distilled water repeatedly until the pH of supernatant was constant, then it was dried at 105 °C for 12 h; ultimately it was ground and sieved using standard mesh to particles with sizes between 0 and 0.15 mm. The obtained AC was characterized by BET analysis using a surface area analyzer (JW-BK122 W, China), a scanning electron microscope (SEM, Hitachi S4800, Japan) and FTIR spectroscopy (Perkin–Elmer "Spectrum BX" spectrometer).

Adsorption experiments

The original solution containing 1.000 g/L of Cr(VI) was prepared by dried $K_2Cr_2O_7$ in a 1,000 mL volumetric flask. According to the demand, it was diluted to acquire standard solutions containing 10, 20, 30, 40 and 50 mg/L of Cr(VI), respectively. The pH of the solution was adjusted to the wide range of 2.5–8 by adding an appropriate amount of

0.1 M HCl or 0.1 M NaOH solutions, which were measured by the Model pHS-3C (pH meter, Shanghai).

Experiments on the effect of adsorbent dosage were carried out by dropping different amounts of AC into Cr(VI) solution with a fixed concentration of 50 mg/L at pH = 2.5. The samples were shaken at room temperature (25 ± 1°) at 150 rpm for 48 h to ensure that sorption equilibrium was reached. Duplicate samples were prepared for all sorption experiments. After equilibrium, the samples were filtered through a 0.45 μm millipore membrane filter. The ion content of Cr(VI) was determined by the UV-5100 spectrophotometer (Shanghai Metash Instruments Co., Ltd, Shanghai, China) at the wavelength of 540 nm, using 1,5-diphenylcarbazide as chromogenic reagent, and H_2SO_4 and H_3PO_4 as buffering agents.

Batch sorption experiments were performed by adding 50 mg carbon into 50 mL Cr(VI) solution to investigate the impact of initial Cr(VI) concentration and initial pH on the sorption. Adsorption kinetic experiments were performed by dispersing a known dose (0.2 g/L) of adsorbents into 1 L Cr(VI) solution with a concentration of 50 mg/L and pH of 2.5 in a glass beaker. The beaker was then agitated on a magnetic stirrer (HJ-3, Jintan Medical Instrument Corporation) at a constant speed of 150 rpm at a temperature of 25 ± 1 °C. The samples were drawn out using an injector at the desired time and filtered with a 0.45 μm membrane filter for analysis, applying the same method described above.

Regeneration studies

The regeneration studies were conducted by batch experiments. Firstly, the optimum initial conditions of Cr(VI) adsorption experiments were implemented as follows: concentration of Cr(VI) solution was 50 mg/L, dosage of adsorbent was 1.0 g/L, temperature was 25 °C, vapour-bathing vibrator was at a rotating speed of 150 rad/min, pH = 2.5 and sorption reaction time was 24 consecutive hours. The AC saturated with Cr(VI) (AC-Cr) was taken out by filtrating the reaction solution and dried at 105 °C for 12 h. Although in theory the Cr(VI) ions were probably reduced to Cr(III) ions at low pH, it has been reported that the amount of total chromium is almost the same as that of Cr(VI) under acidic conditions at low pH (Kumar *et al.* 2007). The results show that the existence of Cr(III) is negligible in the final solution (Gupta & Babu 2009). Therefore, the amount of Cr(III) is not considered in this research.

Four kinds of chemical regeneration agents (RAs) and two concentrations for each RA were selected to conduct the first regeneration cycle (RAs: HNO_3, H_2SO_4, NaOH, NaCl; concentrations: 0.1 and 1.0 mol/L). AC-Cr was divided into several parts, and these parts were added into different RAs with different concentrations at a dosage of 1.0 g/L. Next the samples were shaken at a rotate speed of 150 rad/min for 8 h, then filtrated using vacuum filtration, washed with distilled water for 8–10 times and dried at 110 °C for 12 h. The obtained materials were identified as AC-R, and secondary adsorption experiments were conducted for AC-R by means of the above mentioned procedure. The adsorption-regeneration-adsorption (A-R-A) processes were repeated using the RA which presented the best regeneration performance in the initial adsorption with detailed RA concentrations and regeneration times to explore the effects of RA concentration and regeneration time on regeneration efficiency. The whole experimental procedure is summarized and presented in Figure 1. Each A-R-A procedure with the best RA in the initial adsorption was continued for five cycles using 10% (w/w) HCl as eluent.

The amount of Cr(VI) absorbed at equilibrium by the ACs (q_e, mg/g), the removal rate of Cr(VI) and the percentage of regeneration were calculated respectively by Equations (1)–(3), as follows:

$$q_e = \frac{(C_0 - C_e)V}{W} \tag{1}$$

$$\%\text{Removal} = \frac{100(C_0 - C_i)}{C_0} \tag{2}$$

$$\%\text{Regeneration} = \frac{100(C_0 - C_{e1})}{(C_0 - C_{e2})} \tag{3}$$

where C_0, C_i and C_e are the initial, effluent and equilibrium concentrations (mg/L) of Cr(VI), C_{e1} and C_{e2} are the equilibrium concentration (mg/L) of the initial adsorption and secondary adsorption, V is the volume of Cr(VI) aqueous solution (mL) and W is the amount of AC (g).

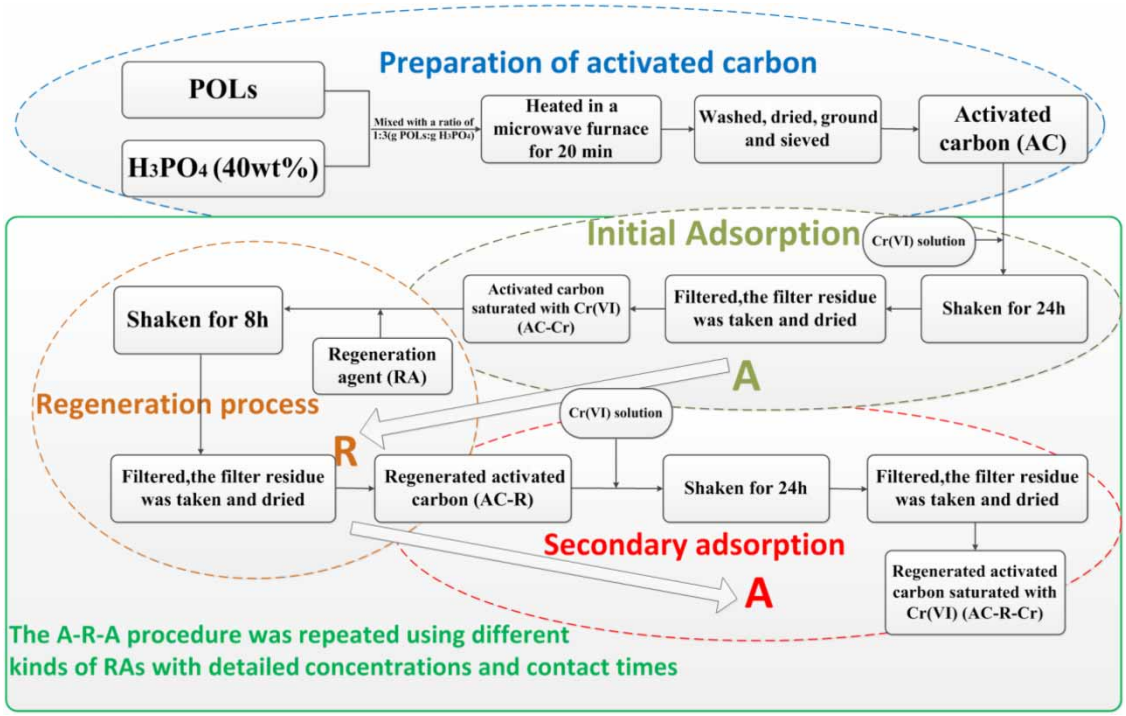

Figure 1 | The flow charts of the experimental procedure in this study.

RESULTS AND DISCUSSION

Characterization of AC

Figure 2 and Table 1 display the characterization results of AC, including SEM images, pore size distribution, N_2 adsorption/desorption isotherms, surface area and pore volume parameters. From the SEM images we can see that the carbon surface was extremely rugged and thickly dotted with irregular pores, indicating that porosity had been well developed during the activation process. Figure 2(a) shows that the distribution of the pores was concentrated and chiefly distributed in the narrow aperture range dimension of 0–1.5 and 2–4 nm. N_2 adsorption/desorption isotherms show a representative type II curve and a type H4 N_2 hysteresis loop, suggesting the coexistence of micropores and mesopores. The S_{mic}/S_{BET}, V_{mic}/V_{tot} values and average pore diameter were 48.2%, 31.1%, 5.442 nm, respectively, demonstrating that AC contained mostly mesopores. The surface area of AC was 1089.67 m^2/g while total pore volume was 1.468 cm^3/g. Compared with those ACs whose S_{BET} is similar, its pore volume is quite high (Liu *et al.* 2012) and is beneficial for enhancing its adsorptive capacity.

Effect of adsorbent dosage on adsorption

The study of the influence of the dosage of adsorbent on Cr(VI) removal was significant enough to give rise to the most appropriate amount of AC, which was guided by an apparent trade-off between the adsorptive capacity and the removal efficiency of Cr(VI) (Gupta & Babu 2009). Figure 3(a) shows the impact of dosage of AC on the adsorption of Cr(VI) when the other adsorption conditions were as follows: concentration of Cr(VI) solution was 50 mg/L, temperature was 25 °C, vapour-bathing vibrator was at a rotating speed of 150 rad/min, pH = 2.5, and sorption reaction time was 24 consecutive hours. The percentage removal increased drastically from 31.39 to 87.94% by increasing the amount of the adsorbent from 0.2 to 1.0 g/L, while the surface adsorption ability reduced from 71.17 to 40.59 mg/g, respectively.

The increase in percentage removal of Cr(VI) with the rise in AC dosage may be due to the increase in

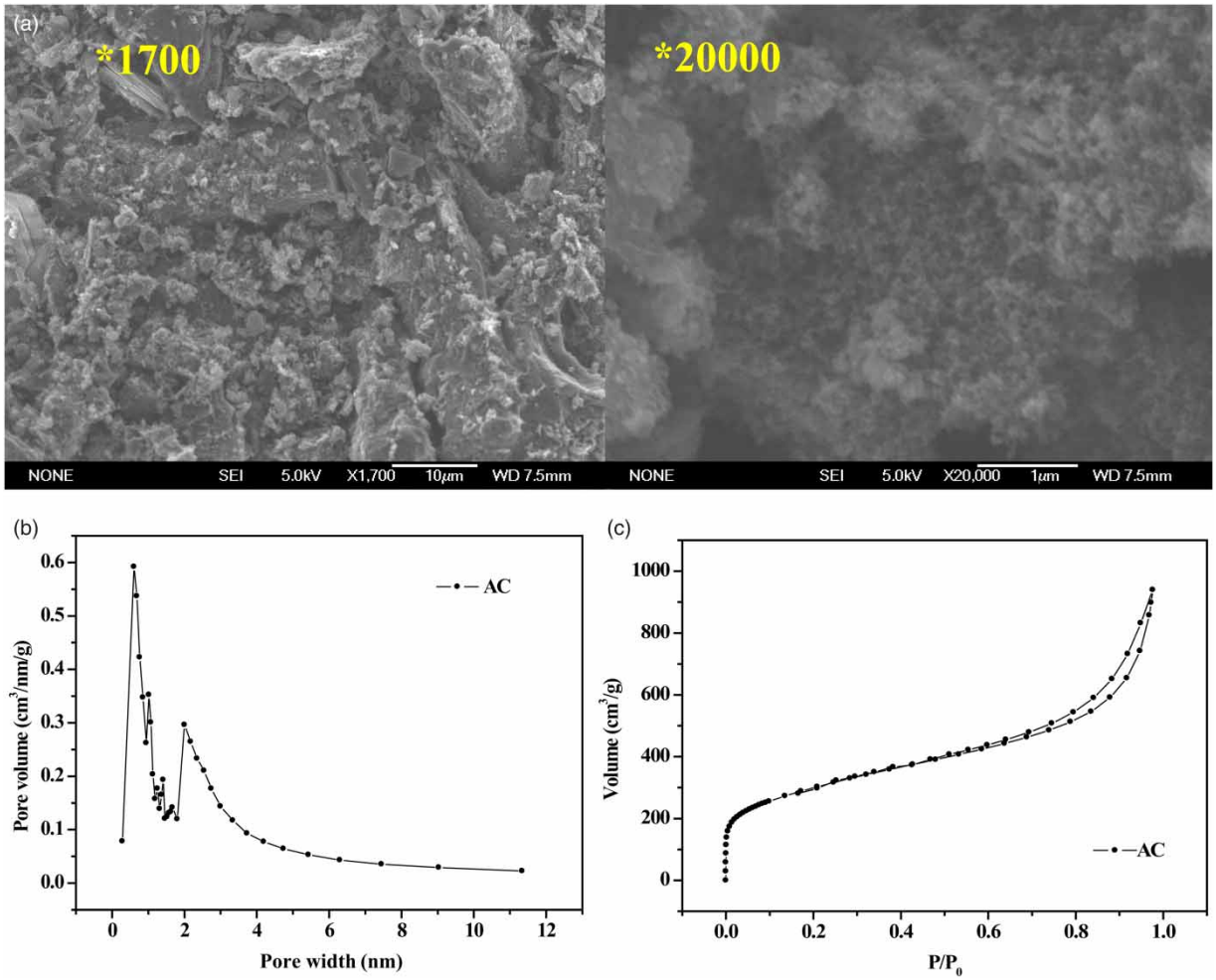

Figure 2 | (a) SEM images, (b) pore size distribution and (c) N_2 adsorption/desorption isotherm of AC.

Table 1 | Surface area and pore volume parameters of AC

	S_{BET} (m^2/g)	S_{ext}		S_{mic}		V_{mic}		V_{tot} (cm^3/g)	D_p (nm)
		(m^2/g)	%	(m^2/g)	%	(cm^3/g)	%		
AC	1089.67	564.62	51.8	525.05	48.2	0.456	31.1	1.468	5.442

S_{BET}, BET surface area; S_{ext}, external surface area; S_{mic}, micropore surface area; V_{mic}, micropore volume; V_{tot}, total pore volume, D_p, average pore diameter.

total surface area and pore volume, namely adding bonding of the Cr(VI) ions to AC. The corresponding mass of Cr(VI) adsorbed per unit mass of adsorbent is referred to as adsorption capacity. The amount of Cr(VI) adsorbed per unit mass of adsorbent consequentially decreased with the increased adsorbent amount on account of the lower available number of Cr(VI) ions under the constant Cr(VI) solution concentration. The unsaturated adsorption sites in the process of physisorption were generated resulting from the increasing of the AC adsorbent dosage; therefore, adsorption capacity decreased.

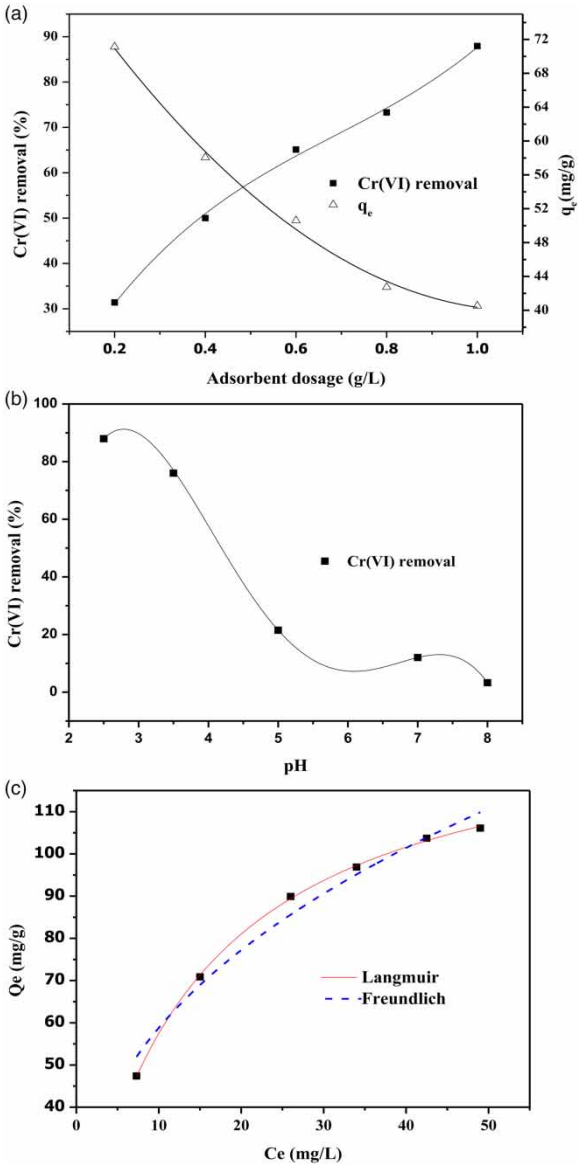

Figure 3 | (a) Effect of dosage of AC on the adsorption of Cr(VI) (initial Cr(VI) concentration: 50 mg/L, initial pH: 2.5, temperature: 25°, reaction time: 24 h), (b) Effect of initial solution pH on the adsorption of Cr(VI) (initial Cr(VI) concentration: 50 mg/L, AC dosage: 1.0 g/L, temperature: 25 °C, reaction time: 24 h) and (c) Adsorption isotherms of Cr(VI) onto AC fitted by Langmuir model and Freundlich model (initial Cr(VI) concentration: 50 mg/L, initial pH: 2.5, temperature: 25 °C, contact time: 24 h).

Effect of pH and initial Cr(VI) concentration on adsorption

The effect of initial pH of the solution on the adsorption process is displayed in Figure 3(b), and the experimental conditions were: pH varied from 2.5 to 8, concentration of Cr(VI) solution was 50 mg/L, temperature was 25 °C, rotating speed was 150 rad/min and sorption reaction time was 24 consecutive hours. The adsorption of metal ions from aqueous solution was influenced by one of the principal elements, which is the value of pH. As can be obviously seen from Figure 3(b), the percentage of Cr(VI) removal decreased keenly with the increased value of pH; in other words, it was strongly pH dependent. When the pH value changed from 2.5 to 8.0, the percentage of Cr(VI) removal was found to decrease from 87.94 to 3.28%, which can be explained as follows: at low pH (2.5–4.0), the dominant species of Cr(VI) in aqueous solution was $HCrO_4^-$ while the superficies of AC were highly protonated and, as a consequence, a forceful attraction existed between $HCrO_4^-$ and the surface of the adsorbent carrying positive charges. As the pH value increased in the range of 4.0–8.0, the metal uptake further decreased, which may be due to the fact that the surface of the substrate is negatively charged at higher pH. This is by virtue of one or both of the following factors. One possibility is the adsorption of hydroxyl ions on the substrate, and another possibility is that the weak acidic functional groups of the adsorbent are ionized (Giri *et al.* 2012). There is a repulsive force generated between the negatively charged surface and the dichromate ions ($Cr_2O_7^{2-}$) or chromate ions (CrO_4^{2-}).

The experimental conditions for the study on the effect of initial concentration of Cr(VI) were: pH = 2.5, concentrations of Cr(VI) solution were from 10 to 100 mg/L, temperature was 25 °C, rotating speed was 150 rad/min and sorption reaction time was 24 consecutive hours. The

Table 2 | Langmuir and Freundlich isothermal adsorption constants for the Cr(VI) sorption on AC

	Langmuir			Freundlich		
Activated carbon	Q_m(mg/g)	K_L(L/mg)	R^2	K_F (mg/g(L/mg)$^{1/n}$)	1/*n*	R^2
AC	135.24	0.0743	0.9934	18.30	0.4767	0.9796

adsorption capacity was obtained from the isotherm study which applied the Langmuir and Freundlich isothermal adsorption models, shown in Figure 3(c), and the Langmuir model was the best to represent the records with high R^2 (>0.99). The fitted constants are shown in Table 2. Therefore, the uptake of Cr (VI) by AC may involve a monolayer adsorption with interactions between the adsorbed molecules. The calculated adsorption capacity was 135.24 mg/g. Table 3 displays a comparison of the maximum adsorption capacities and the preparation process of different adsorbents for Cr(VI). Compared with other adsorbents, the survey consequences of the current research manifest that the POLs-based AC has a better adsorption capacity and can be used as a preferable adsorbent for the removal of Cr(VI) from liquid waste.

Effect of contact time on adsorption and kinetics

Effect of contact time on adsorption was investigated with the conditions as follows: concentration of Cr(VI) solution was 50 mg/L, dosage of adsorbent was 0.2 g/L, pH = 2.5, temperature was 25 °C, rotating speed was 150 rad/min, and the results are shown in Figure 4. As can be seen from the figure, the concentration of Cr(VI) reduced rapidly in the first 20 min, then the reduced rate slowed down gradually, and the concentration became near constant after 100 min. Eventually, equilibrium was achieved in 2 h. The mechanism of Cr(VI) shifting to the adsorbent included two stages: diffusing through the fluid membrane around the AC particles and diffusing through the pore structure to the interior active sites. In the first step, the gradient concentration for Cr(VI) ions between the available surface active sites and the fluid film was large, so the transfer of Cr(VI) was faster. The removal rate of Cr(VI) decreased in the later stage because the intraparticle diffusion became dominant, and this may be due to the slow pore diffusing of Cr(VI) into the bulk of the adsorbent. Herein, Cr(VI) particles took more time to move from the surface of the solid to the interior adsorption sites through the pores.

For the purpose of studying the adsorption dynamics mechanism of Cr(VI) ions on AC, three dynamical models, pseudo-first order kinetic model, pseudo-second order kinetic model and intraparticle diffusion model, were applied in this study. Figure 5 displays the equation fitting diagrams of the above three models. The kinetic parameters of those three models for Cr(VI) adsorption on the surface of AC were counted and are summarized in Table 4. The gained coefficients of correlation (R^2) imply that the experimental data is more consistent with the pseudo-second order dynamics model, in which R^2 can reach up to 0.9987. Moreover, the calculated adsorption amount $q_{e,cal}$ (mg/g) fits well with experimental $q_{e,exp}$. These results imply that the process of adsorption was

Table 3 | Maximum adsorption capacities and the preparation process of different carbon adsorbents for Cr(VI)

		Preparation process				
Adsorbent	**q_{max} (mg/g)**	**Temperature (°C)**	**Heating time**	**Optimum pH**	**Agent**	**References**
Sugarcane bagasse carbon	103	180	2 h	3.0	DMDHEU and choline chloride	Wartelle & Marshall (2005)
Sawdust activated carbon	65.8	364	1 h	2.0	H_3PO_4	Karthikeyan *et al.* (2005)
Rice husk carbon	48.31	150	24 h	2.0	H_2SO_4	Bansal *et al.* (2009)
Activated tamarind seeds	29.7	150	24 h	2.0	H_2SO_4	Gupta & Babu (2009)
Ficus carica fibre AC	44.84	700	5 min	3.0	H_3PO_4	Gupta *et al.* (2013)
Corn cob AC/magnetite	57.37	500	2 h	2.0	$FeSO_4$	Nethaji *et al.* (2013)
Acrylonitrile-divinylbenzene	80	850	–	2.0	Air	Duranoğlu *et al.* (2012)
AC	135.24	450°C	20 min	2.5	H_3PO_4	This study

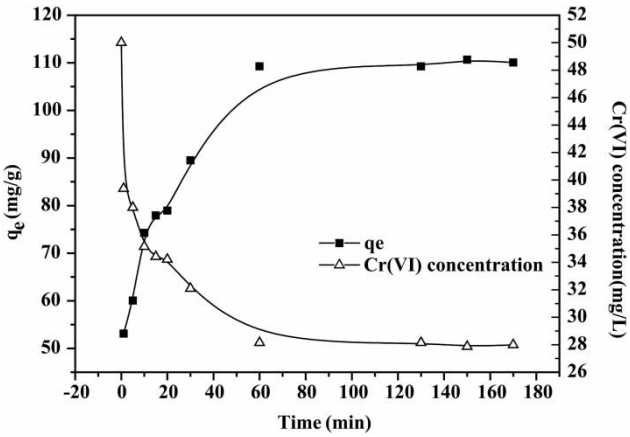

Figure 4 | Effect of contact time on Cr(VI) adsorption (initial Cr(VI) concentration: 50 mg/L, AC dosage: 1.0 g/L , initial pH: 2.5, temperature: 25 °C).

affected and controlled by chemisorption (Hameed 2009) and electrostatic interactions (Huang *et al.* 2011).

For the purpose of carrying out further research on the mechanisms and adsorption rate controlling steps influencing the kinetics, the model of intraparticle diffusing was used in this study about the steps of rate controlling. Figure 5(c) shows that the data of adsorption presents multi-linear plots with two steps. The first portion of the curve does not pass through the original point, which illustrates that the speed is not only controlled by particle internal diffusion but also by other different mechanisms such as boundary layer diffusion.

As can be seen from the intraparticle diffusion plot, the first linear part of the curve implies that Cr(VI) adsorption is controlled by external film resistance or external mass transfer. For the second section of the curve, intraparticle diffusing was limited by rate, and eventually the state of equilibrium was approached. The intraparticle diffusion rate began to decrease as a result of the following points: (a) the Cr(VI) concentration was decreasing; (b) the pore diameter for diffusion was smaller; (c) the electrostatic repulsion on the surface of AC was intensified (Liu *et al.* 2011).

The $k_{int\ i}$ and $C_{int\ i}$ values can reveal the rate of the adsorption process and the boundary layer thickness. The $k_{int\ i}$ value severely decreased and the $C_{int\ i}$ value increased as time passed in the process of adsorption. Taking the effect of time into consideration, it was put forward that intraparticle diffusion plays a critical part in the process of adsorption (Liu *et al.* 2011).

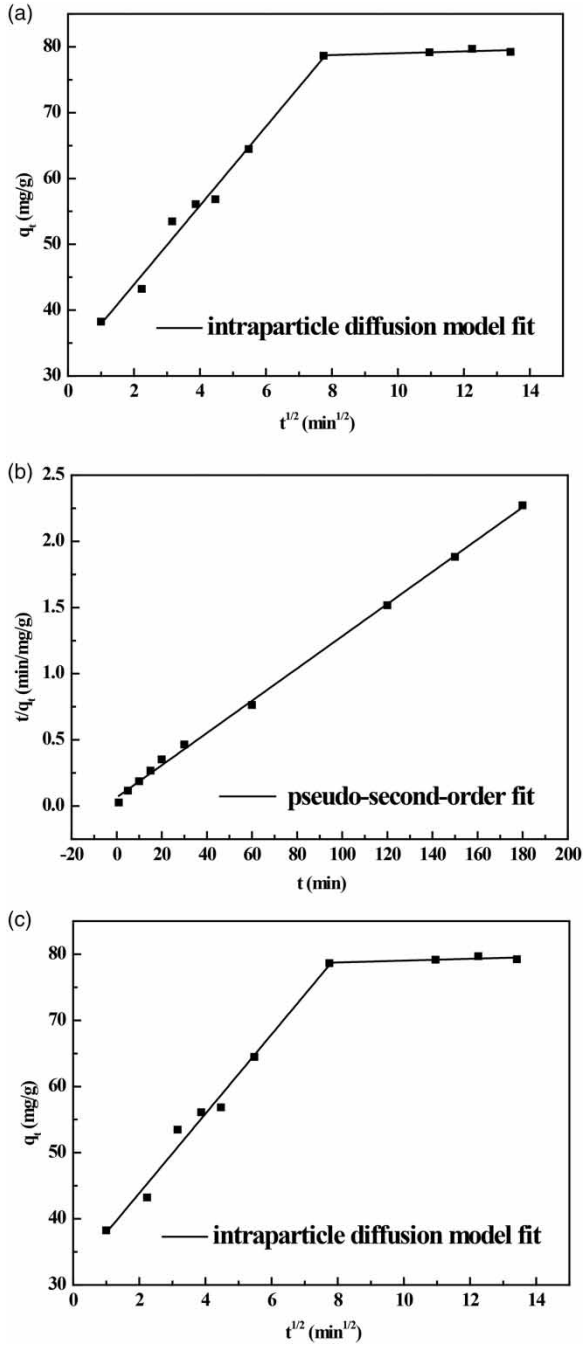

Figure 5 | The curves of (a) pseudo-first order model, (b) pseudo-second order model and (c) intraparticle diffusion model for the removal of Cr(VI) by AC.

Regeneration studies

For the sake of a sustainable adsorption process, the adsorbents should have the potential of superb desorption and reusability. Regeneration studies help to determine the

Table 4 | Kinetic parameters of pseudo-first order model, pseudo-second order model and intraparticle diffusion model for the removal of Cr(VI) by AC

Kinetic models	Parameters	Values
Pseudo-first order model	$q_{e,exp}$ (mg/g)	79.65
	$q_{e,\ cal}$ (mg/g)	56.70
	k_1 (mg/g min)	0.06130
	R^2	0.9258
Pseudo-second order model	$q_{e,exp}$ (mg/g)	79.65
	$q_{e,\ cal}$ (mg/g)	81.96
	$k_2 \times 10^{-3}$ (mg/g min)	2.300
	R^2	0.9987
Intraparticle diffusion model	K_{int1}	6.0022
	$C_{int\ 1}$	31.88
	R_1^2	0.9821
	K_{int2}	0.1380
	$C_{int\ 2}$	77.65
	R_2^2	0.4681

k_1 (1/h) and k_2 (g/(mg h)) are the rate constants of pseudo-first order and pseudo-second order model, respectively; $K_{int\ 1}$ (mg(g $h^{1/2})^{-1}$) and $K_{int\ 2}$ are the intraparticle diffusion rate constants of the first and second stage in intraparticle diffusion model, $C_{int\ 1}$ and $C_{int\ 2}$ are the slopes of the first and second stage in intraparticle diffusion model.

adsorption mechanism and to evaluate the feasibility of reusing the spent AC (Liu *et al.* 2010).

Regeneration performances of four kinds of RAs

HNO_3, H_2SO_4, NaOH and NaCl were selected to perform the first round of the A-R-A procedure. The regeneration performances of the four chemical RAs are illustrated in Figure 6(a).

From the results displayed in Figure 6(a), NaOH and NaCl were not suitable for the regeneration of AC-Cr due to their poor regeneration performances. Meanwhile, H_2SO_4 and HNO_3 exhibited relatively high percentages of regeneration but the latter was better; therefore, acidic RAs were adaptive for the regeneration of ACs saturated with chrome. Herein HNO_3 was chosen to conduct the A-R-A procedure again to explore the optimum regeneration conditions and mechanism.

Regeneration of AC-Cr by HNO_3 and regeneration mechanism

Figure 6(b) and 6(c) demonstrate the influence of HNO_3 concentration and regeneration time on the percentage of regeneration. The regeneration performance for AC-Cr increased at the initial stage and then decreased with the rise of HNO_3 concentration; the culminating point appears at the 20% concentration with a% regeneration of 55.42%. This phenomenon may be explained as follows: the regeneration effect of HNO_3 for AC-Cr can be assigned to three aspects: (a) a number of new functional groups (such as N-H bond, see below under FTIR analysis of AC, AC-Cr, AC-R, AC-R-Cr and adsorption mechanism) were introduced onto the surface of AC by molecules of HNO_3, which accordingly increased the surface activation sites; (b) due to the strong oxidizing property and acidity of HNO_3, it can corrode and drill plenty of new pores and holes inside the carbon; (c) HNO_3 reacts chemically with Cr(VI), which was adsorbed onto the AC surface, promoting the desorption process. When the concentration of HNO_3 increased from 0 to 20%, the above mentioned three aspects all resulted in positive roles, but with the rise of the concentration, excessive HNO_3 was added into the system, the above (a) and (c) effects tended to approach an equilibrium state and no longer increased, the (b) effect took advantage, the porosity of AC was overly corroded and partly destroyed, and therefore the regeneration performance accordingly degraded. It can be clearly seen from Figure 6(c) that the regeneration reaction mainly arose in the first 1.5 h and could reach equilibrium within 4 h. The %regeneration-regeneration time curve can provide information on the optimum regeneration time, which was 4 h in the present case.

However, in general, the regeneration rate was not ideal, with a maximum value of 55.42%; these findings imply that the mechanism of Cr(VI) adsorption onto AC is predominantly chemisorption, and the Cr(VI) ions may have formed strong bonds with the adsorbent surface, which was in keeping with the results of the aforementioned kinetic study.

In addition, the major problem of the regeneration process is the disposition of the regeneration solution acquired, which contains Cr(VI) in high concentration. Gupta & Babu (2009) suggested a method to address this issue which uses barium chloride to produce one precipitation of Cr(VI) from the aqueous solution. The bright yellow barium chromate precipitate was generated by adding a barium chloride solution to the Cr(VI) solution, which can be reused by the industries.

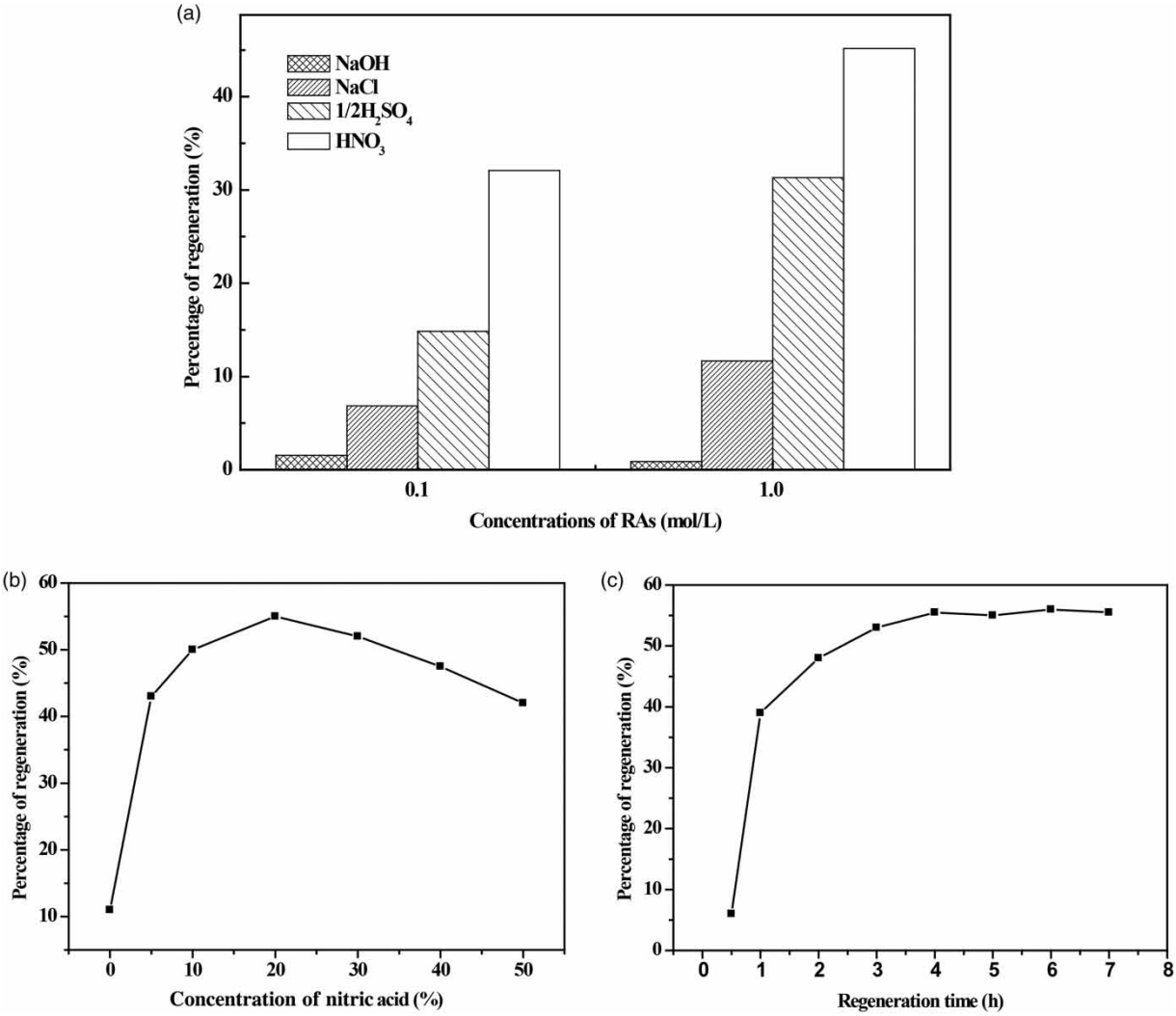

Figure 6 | (a) Regeneration performances of HNO_3, $1/2H_2SO_4$, NaOH and NaCl after one regeneration cycle, (b) influence of concentration of HNO_3 on the percentage of regeneration with five regeneration cycles and (c) influence of regeneration time on the percentage of regeneration after one regeneration cycle.

FTIR analysis of AC, AC-Cr, AC-R, AC-R-Cr and adsorption mechanism

The FTIR spectra (400–4,000 cm^{-1}) of ACs are shown in Figure 7. The broad bands at around 3,416, 1,619, 1,181 and 492 cm^{-1} are the results of the stretching vibration of –OH, C = C or C = O, C–C or C–O and S–S functionalities, respectively. Noteworthily, the peak was located at 2,922 cm^{-1}, which is attributed to the N-H bond on the AC-Cr sample's spectrum being larger than that of other samples, suggesting that HNO_3 successfully introduced the N-H bond onto the AC surface in the regeneration process.

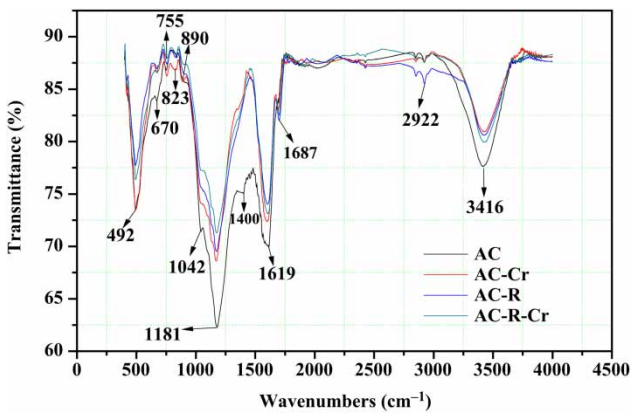

Figure 7 | FTIR spectra of AC, AC-Cr, AC-R and AC-R-Cr.

The obtained FTIR spectra (400–4,000 cm^{-1}) of ACs also reveal that the species of functional groups of AC did not change obviously during the A-R-A process, but the quantities of most groups reduced markedly after initial adsorption, indicating that the disappeared functional groups were occupied by Cr(VI) and chemisorption

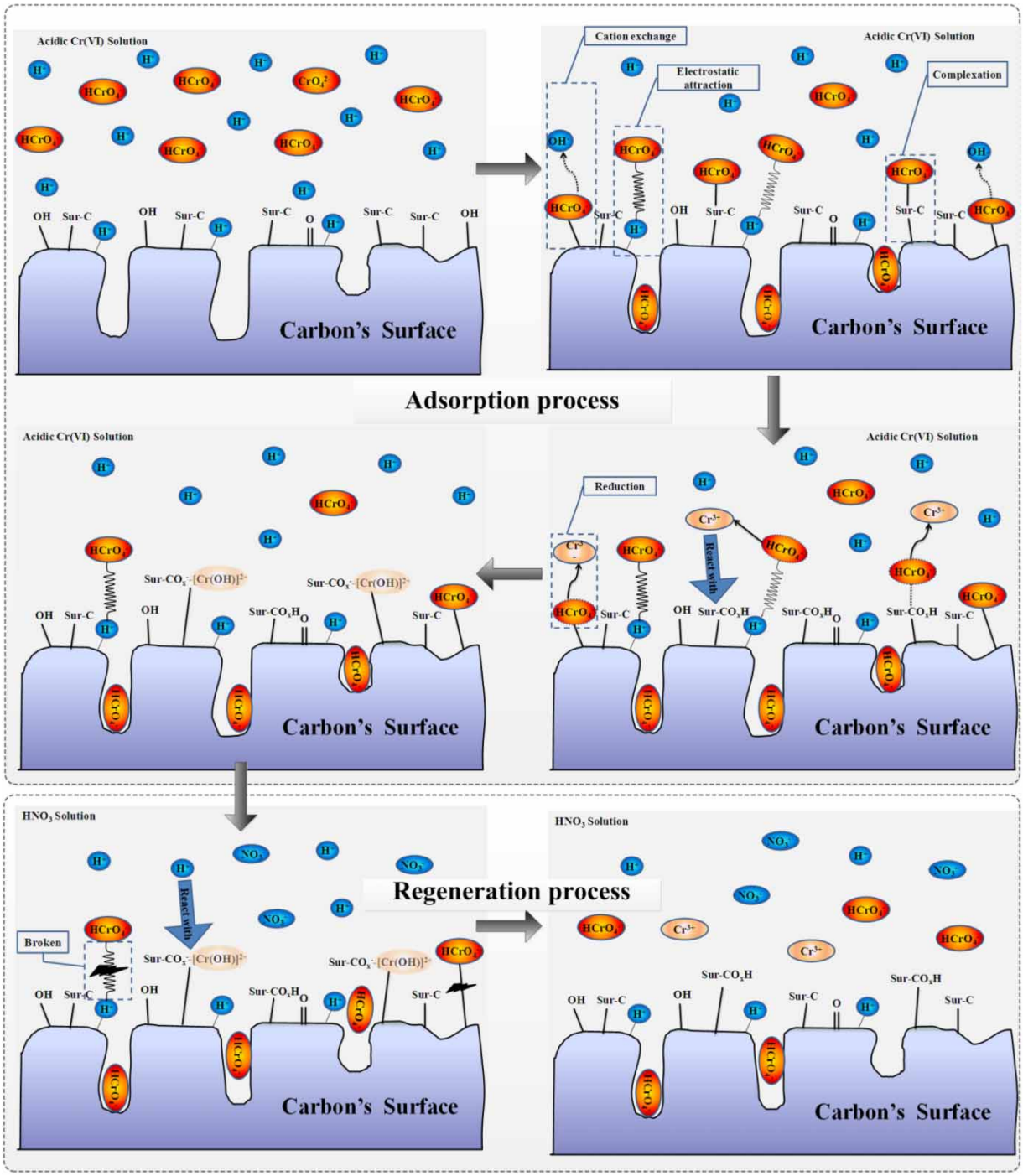

Figure 8 | Graphical representation of the adsorption and regeneration mechanism.

occurred, which corresponds with the results of the kinetic study; see above under Effect of contact time on adsorption and kinetics. The dominant species of Cr(VI) in the aqueous solution is $HCrO_4^-$ at low pH. There are three stages in the mechanism of the adsorption: the absorption and loading of chromate on the AC surface, the Cr reduced from Cr(VI) to Cr(III), and the ionic exchange of Cr(III) with oxygen functional groups which are original or newly formed on the AC surface, just as shown below (Huang *et al.* 2014):

$$HCrO_4^- + 7H^+ + 3e^- \leftrightarrow Cr^{3+} + 4H_2O \quad (4)$$

$$CrO_4^{2-} + 8H^+ + 3e^- \leftrightarrow Cr^{3+} + 4H_2O \quad (5)$$

$$Sur - C - e^- \leftrightarrow Sur - CO_xH \quad (6)$$

$$Cr^{3+} + H_2O + Sur - CO_xH \leftrightarrow (Sur - CO_x^- - [Cr(OH)]^{2+}) + 2H^+ \quad (7)$$

in which Sur-C stands for the C bond on the surface of AC, and Sur-CO_xH is characteristic of the newly formed oxygenic functional groups. To further understand the process as well as to realize the characteristics of the material which contribute to designing a new adsorbent for future applications, the mechanism of any adsorption process is a significant constituent part (Giri *et al.* 2012). A brief graphical representation of the adsorption and regeneration mechanism is shown in Figure 8.

CONCLUSIONS

In this study, AC was prepared from *Platanus orientalis* leaves by H_3PO_4 activation using a microwave heating method; this carbon exhibited a surface area of 1089.67 m^2/g and a relatively high pore volume of 1.468 cm^3/g. Utilization of this carbon for the Cr(VI) ions removal from aqueous solution is surveyed in the current research. It was discovered that the adsorption was strongly pH dependent and equilibrium could be reached in 2 h. The maximum adsorption of Cr(VI) calculated from the isotherm study can reach the relatively high value of 135.24 mg/g. In the kinetic study, it is found that the adsorption of Cr(VI) obeyed the pseudo-second order model ($R^2 > 0.99$), which implies that chemisorption had control of the adsorption process. The intraparticle diffusion model was applied to inquire into the adsorption rate controlling step, and the results show that intraparticle diffusion is not the only rate controlling procedure. HNO_3 displayed the best regeneration performance of the four chemical RAs; the regeneration performance increased at first and then decreased with the rise of HNO_3 concentration, and regeneration reaction can reach equilibrium within 4 h. The FTIR spectra reveal that HNO_3 successfully introduced an N-H bond onto the AC surface in the regeneration process.

ACKNOWLEDGEMENTS

We are grateful to the Fundamental Research Funds of Shandong University (No. 2016JC003) for financial support as well as the contributions of every author to the study.

COMPLIANCE WITH ETHICAL STANDARDS

The authors declare that they have no conflict of interest.

REFERENCES

Aljeboree, A. M., Alshirifi, A. N. & Alkaim, A. F. 2017 Kinetics and equilibrium study for the adsorption of textile dyes on coconut shell activated carbon. *Arab. J. Chem.* **10**, S3381–S3393.

Bansal, M., Singh, D. & Garg, V. 2009 A comparative study for the removal of hexavalent chromium from aqueous solution by agriculture wastes' carbons. *J. Hazard. Mater.* **171** (1), 83–92.

Chen, J., Qin, Y., Chen, Z., Yang, Z., Yang, W. & Wang, Y. 2016 Gas circulating fluidized beds photocatalytic regeneration of I-TiO2 modified activated carbons saturated with toluene. *Chem. Eng. J.* **293**, 281–290.

Duranoğlu, D., Trochimczuk, A. W. & Beker, U. 2012 Kinetics and thermodynamics of hexavalent chromium adsorption onto activated carbon derived from acrylonitrile-divinylbenzene copolymer. *Chem. Eng. J.* **187**, 193–202.

Giri, A. K., Patel, R. & Mandal, S. 2012 Removal of Cr (VI) from aqueous solution by Eichhornia crassipes root biomass-derived activated carbon. *Chem. Eng. J.* **185–186**, 71–81.

Gupta, S. & Babu, B. V. 2009 Utilization of waste product (tamarind seeds) for the removal of Cr(VI) from aqueous

solutions: equilibrium, kinetics, and regeneration studies. *J. Environ. Manage.* **90** (10), 3013–3022.

Gupta, V. K., Pathania, D., Sharma, S. & Singh, P. 2013 Preparation of bio-based porous carbon by microwave assisted phosphoric acid activation and its use for adsorption of Cr(VI). *J. Colloid Interface Sci.* **401**, 125–132.

Hameed, B. H. 2009 Spent tea leaves: a new non-conventional and low-cost adsorbent for removal of basic dye from aqueous solutions. *J. Hazard. Mater.* **161** (2–3), 753–759.

Huang, L., Sun, Y., Wang, W., Yue, Q. & Yang, T. 2011 Comparative study on characterization of activated carbons prepared by microwave and conventional heating methods and application in removal of oxytetracycline (OTC). *Chem. Eng. J.* **171** (3), 1446–1453.

Huang, L., Xue, J., Jin, F., Zhou, S., Wang, M., Liu, Q. & Huang, L. 2014 Study on mechanism and influential factors of the adsorption properties and regeneration of activated carbon fiber felt (ACFF) for Cr(VI) under electrochemical environment. *J. Taiwan Inst. Chem. Eng.* **45** (6), 2986–2994.

Ihsanullah, Al-Khaldi, F. A., Abu-Shark, B., Abulkibash, A. M., Qureshi, M. I., Laoui, T. & Atieh, M. A. 2016 Effect of acid modification on adsorption of hexavalent chromium (Cr(VI)) from aqueous solution by activated carbon and carbon nanotubes. *Desal. Water Treat.* **57** (16), 7232–7244.

Karthikeyan, T., Rajgopal, S. & Miranda, L. R. 2005 Chromium (VI) adsorption from aqueous solution by Hevea Brasilinesis sawdust activated carbon. *J. Hazard. Mater.* **124** (1), 192–199.

Kaushik, A., Basu, S., Singh, K., Batra, V. S. & Balakrishnan, M. 2017 Activated carbon from sugarcane bagasse ash for melanoidins recovery. *J. Environ. Manage.* **200**, 29–34.

Köseoğlu, E. & Akmil-Başar, C. 2015 Preparation, structural evaluation and adsorptive properties of activated carbon from agricultural waste biomass. *Adv. Powder Technol.* **26** (3), 811–818.

Kumar, P. A., Ray, M. & Chakraborty, S. 2007 Hexavalent chromium removal from wastewater using aniline formaldehyde condensate coated silica gel. *J. Hazard. Mater.* **143** (1–2), 24–32.

Li, Q., Qi, Y. & Gao, C. 2015 Chemical regeneration of spent powdered activated carbon used in decolorization of sodium salicylate for the pharmaceutical industry. *J. Clean. Prod.* **86**, 424–431.

Liu, W., Zhang, J., Zhang, C., Wang, Y. & Li, Y. 2010 Adsorptive removal of Cr (VI) by Fe-modified activated carbon prepared from trapa natans husk. *Chem. Eng. J.* **162** (2), 677–684.

Liu, H., Liu, W., Zhang, J., Zhang, C., Ren, L. & Li, Y. 2011 Removal of cephalexin from aqueous solutions by original and Cu(II)/Fe(III) impregnated activated carbons developed from lotus stalks Kinetics and equilibrium studies. *J. Hazard. Mater.* **185** (2–3), 1528–1535.

Liu, F., Chuang, S., Oh, G. & Seo, T. S. 2012 Three-dimensional graphene oxide nanostructure for fast and efficient water-soluble dye removal. *ACS Appl. Mater. Interfaces* **4** (2), 922–927.

Liu, C., Sun, Y., Wang, D., Sun, Z., Chen, M., Zhou, Z. & Chen, W. 2017 Performance and mechanism of low-frequency ultrasound to regenerate the biological activated carbon. *Ultrasonics Sonochem.* **34**, 142–153.

Mao, H., Zhou, D., Hashisho, Z., Wang, S., Chen, H. & Wang, H. H. 2015 Constant power and constant temperature microwave regeneration of toluene and acetone loaded on microporous activated carbon from agricultural residue. *J. Ind. Eng. Chem.* **21**, 516–525.

Nethaji, S., Sivasamy, A. & Mandal, A. B. 2013 Preparation and characterization of corn cob activated carbon coated with nano-sized magnetite particles for the removal of Cr(VI). *Bioresour. Technol.* **134**, 94–100.

Oh, W.-D., Lua, S. K., Dong, Z. & Lim, T. T. 2015 Performance of magnetic activated carbon composite as peroxymonosulfate activator and regenerable adsorbent via sulfate radical-mediated oxidation processes. *J. Hazard. Mater.* **284**, 1–9.

Wartelle, L. H. & Marshall, W. E. 2005 Chromate ion adsorption by agricultural by-products modified with dimethyloldihydroxyethylene urea and choline chloride. *Water Res.* **39** (13), 2869–2876.

Yang, K., Peng, J., Srinivasakannan, C., Zhang, L., Xia, H. & Duan, X. 2010 Preparation of high surface area activated carbon from coconut shells using microwave heating. *Bioresour. Technol.* **101** (15), 6163–6169.

First received 12 March 2018; accepted in revised form 21 June 2018. Available online 23 July 2018